AD-A083 723 PURDUE UNIV LAFAYETTE IND PROJECT SQUID HEADQUARTERS F/G 21/2
SECOND-ORDER CLOSURE MODELING OF VARIABLE DENSITY TURBULENT FLO--ETC(U)
MAR 79 A K VARMA, P J MANSFIELD, G SANDRI N00014-75-C-1143
UNCLASSIFIED SQUID-ARAP-2-PU NL

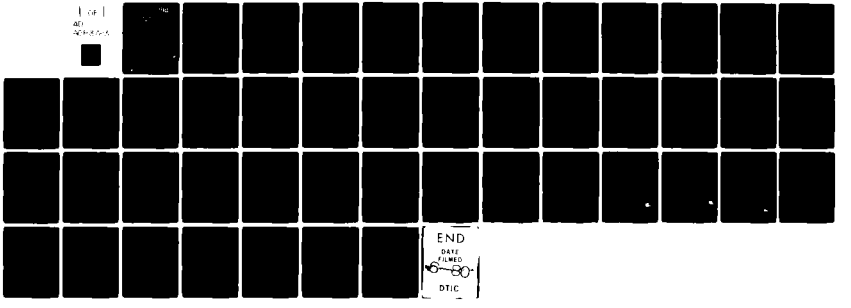

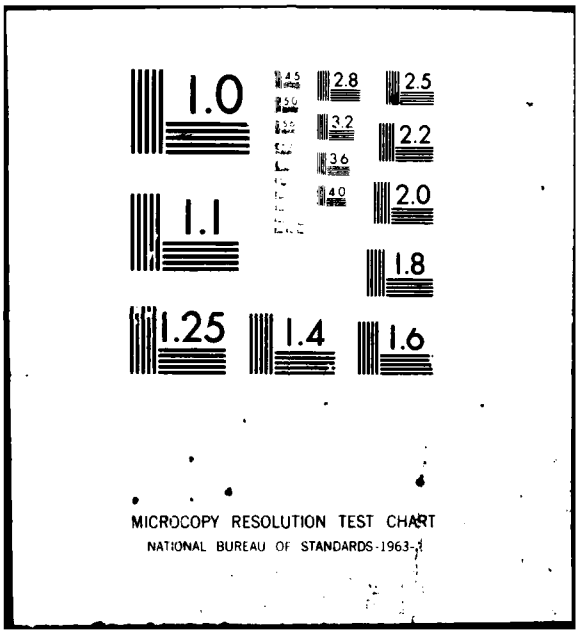
1.0
1.1
1.25
1.4
1.6
1.8
2.0
2.2
2.5
2.8
3.2
3.6
4.0
MICROCOPY RESOLUTION TEST CHART
NATIONAL BUREAU OF STANDARDS-1963-A

PROJECT SQUID

TECHNICAL REPORT ARAP-2-PU

SECOND-ORDER CLOSURE MODELING OF VARIABLE DENSITY TURBULENT FLOWS

ASHOK K. VARMA, PETER J. MANSFIELD and GUIDO SANDRI
AERONAUTICAL RESEARCH ASSOCIATES OF PRINCETON, INC.
50 WASHINGTON ROAD, P.O. BOX 2229
PRINCETON, NEW JERSEY 08540

MARCH 1979

Project SQUID is a cooperative program of basic research relating to Jet Propulsion. It is sponsored by the Office of Naval Research and is assisted by Purdue University through Contract N00014-75-C-1143, NR-098-038.

Published for ONR by
School of Mechanical Engineering
Chaffee Hall
Purdue University
West Lafayette, Indiana 47907

Technical Report ARAP-2-PU

P R O J E C T S Q U I D

A COOPERATIVE PROGRAM OF FUNDAMENTAL RESEARCH
AS RELATED TO JET PROPULSION
OFFICE OF NAVAL RESEARCH, DEPARTMENT OF THE NAVY

CONTRACT N00014-77-C-1143, NR-098-038

SECOND-ORDER CLOSURE MODELING OF VARIABLE DENSITY TURBULENT FLOWS

by

Ashok K. Varma[1], Peter J. Mansfield[2] and Guido Sandri[3]
Aeronautical Research Associates of Princeton, Inc.
50 Washington Road, P.O. Box 2229
Princeton, New Jersey 08540

March 1979

Published for ONR by
School of Mechanical Engineering
Purdue University
West Lafayette, Indiana 47907

[1]Consultant
[2]Senior Staff
[3]Senior Consultant

SUMMARY

Mixing and chemical reactions under turbulent flow conditions are a basic feature of the energy release processes in many combustion and propulsion systems. The development of predictive calculation procedures for these systems requires the understanding and modeling of coupling between turbulence and various physical and chemical processes. Second-order closure modeling of turbulent flows provides a rational framework for studying these interactions.

Models for the scalar probability density function (pdf) have to be developed to achieve closure of turbulent transport equations for mixing and reacting flows. A delta function "typical eddy" pdf model for two species flows has been developed and incorporated into a complete second-order closure computer program. The program has been used to study uniform and variable density flowfields and the model predictions have been compared to experimental measurements. The modeling of turbulence dynamics for variable density flows requires further improvement. However, the importance of modeling the higher-order scalar correlations has been demonstrated.

A number of statistical constraints on three species flowfields have also been derived. These will be useful in the development of the "typical eddy" pdf model for reacting flows.

TABLE OF CONTENTS

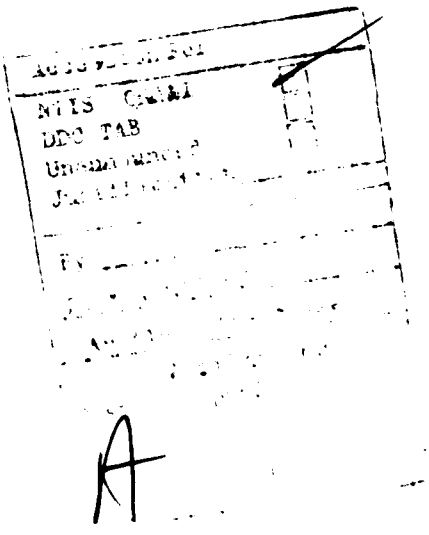

LIST OF FIGURES

1. INTRODUCTION

Mixing and chemical reactions under turbulent flow conditions are a basic feature of the energy release processes in gas turbine combustors and other propulsion systems, and any predictive modeling of the flowfield has to properly account for the effects of the turbulence of the flow and its interactions with various physical and chemical processes. There are significant interaction effects of the turbulence on combustion and of the combustion on the turbulence, which are important in determining combustion efficiency, pollutant formation, combustion noise, heat transfer, etc. Second-order closure modeling of turbulent flows provides a convenient framework for studying these interactions and holds promise of providing a reliable predictive computational tool for the design of new systems and improvement of existing combustion systems.

The modeling of turbulent flows with variable density and combustion requires the development of models for third- and higher-order scalar correlations or, alternately, a model for the joint scalar probability density function (pdf). The development of a satisfactory scalar pdf model is one of the major objectives of this research effort. A "typical eddy" pdf model composed of delta functions has been proposed, and a model for two species variable density mixing flows has been constructed and extensively tested by comparison with measured pdf's in a variable density shear layer flow (Varma et al., 1978).

This pdf model has been incorporated in a complete second-order closure computer program developed at A.R.A.P. The code is designed for multispecies turbulent reacting flows and solves a set of 27 coupled, parabolic partial differential equations for the mean variables and various independent second-order correlations. The second-order closure program with the scalar pdf model has been used to study uniform and variable density planar shear layer flows and a variable density axisymmetric jet flowfield. The program predictions are compared to experimental measurements in this report (Section 2), and the importance of modeling the higher-order scalar correlations has been demonstrated.

The development and testing of a delta function pdf model for three species is also continuing. Various statistical constraints on correlations for three species that have been derived up to now are presented in Section 3 of this report.

2. MODEL VERIFICATION

Uniform and Variable Density Planar Shear Layers

Detailed measurements of the mean velocity $\bar{u}$, mean density $\bar{\rho}$, mean species mole fraction $\bar{c}$, species correlation $\overline{c'c'}$, and species probability density functions (pdf's) in uniform density and variable density planar shear layers have been made by Prof. Roshko and his colleagues at Cal Tech. The data has been reported by Brown and Roshko (1974) and Konrad (1976). The data appears to be the only comprehensive set of measurements for second-order species correlations and scalar pdf's in shear layer flows and should provide a test for turbulence modeling calculations. However, as discussed later, the data has some unexplained anomalies that reduce its value for model verification.

The A.R.A.P. multiequation second-order closure code for shear layer flows has been used to calculate the flowfield for Helium + Argon - Nitrogen (constant density) and Helium - Nitrogen (density ratio = 7) planar shear layers. The velocity ratio for both flows is 0.38. The computations are started at the exit plane of the splitter plate with smooth, monotonic initial profiles of velocity and species concentrations. The initial wall boundary layers are neglected as we are mainly interested in comparison of predictions and experimental data in the downstream fully developed region of the flow. A triangular profile spot of turbulence is introduced at the initial station with $\overline{u'u'} = \overline{v'v'} = \overline{w'w'} = 2|\overline{u'v'}|$. The peak value of $\overline{u'u'} = 0.01(\Delta\bar{u})^2$. Previous studies have

shown that with reasonable profiles, downstream results are quite insensitive to the width and amplitude of the initial turbulence distribution.

Calculations have been carried out using the complete "typical eddy" pdf model including density fluctuations. For comparison purposes, calculations were also made using a pdf "model" in which all third- and higher-order scalar correlations are set to zero. This procedure has been termed the "second-order approximation."

Constant Density Shear Layer Studies

For nonreacting constant density flows the transport equations for the means and the second-order correlations do not contain any third-order scalar correlation terms. Therefore, the results obtained using the "second-order approximation" and the "typical eddy" model are identical.

Analysis of Data. Brown and Roshko (1974) reported measurements of mean velocity profiles in air-air mixing layers with a velocity ratio of 0.38. A standard measure of shear layer spread rate is the parameter σ_o .

$$\sigma_o = 1.855 \frac{x_2 - x_1}{y_2 - y_1} \cdot \frac{\bar{u}_1 - \bar{u}_2}{\bar{u}_1 + \bar{u}_2}$$

y_2 and y_1 are the profile widths corresponding to the 10% and 90% velocity profile points at two axial positions x_2 and x_1 . $\bar{u}_1$ and $\bar{u}_2$ are the freestream velocities in the two streams. We have calculated the parameter σ_o from the Brown and Roshko data and $\sigma_o = 9.7$. This

value is in good agreement with other shear layer data (Birch and Eggers, 1973) wherein σ_0 ranges between 9 and 11, with 11 being the preferred value.

Konrad (1976) reported measurements in a uniform density shear layer composed of streams of He + Ar and N_2 in the same apparatus at similar velocity values, and σ_0 calculated from his measurements has a value of only 7.5; that is, the shear layer is spreading too rapidly. This discrepancy in the spread rate between Konrad (1976) and Brown and Roshko (1974) (and other data in the literature) has to be resolved before one can make full use of the turbulence correlations and pdf measurements of Konrad.

Second-Order Closure Calculations. The predictions for the mean velocity, mean species, and species correlation profiles in the downstream similarity region are compared to the Konrad (1976) data in Figure 1. These calculations use the standard A.R.A.P. model constants that have been established in the past by detailed comparison with basic incompressible jet, wake, shear layer, and flat plate boundary layer flows. The multiequation turbulent reacting code (METREC) uses an algebraic specification of the turbulent macroscale Λ.

$$\Lambda = C \cdot \left| y_{q^2_{max}} - y_{q^2 = \frac{1}{4} q^2_{max}} \right|$$

$C = 0.6$ for shear layer flows

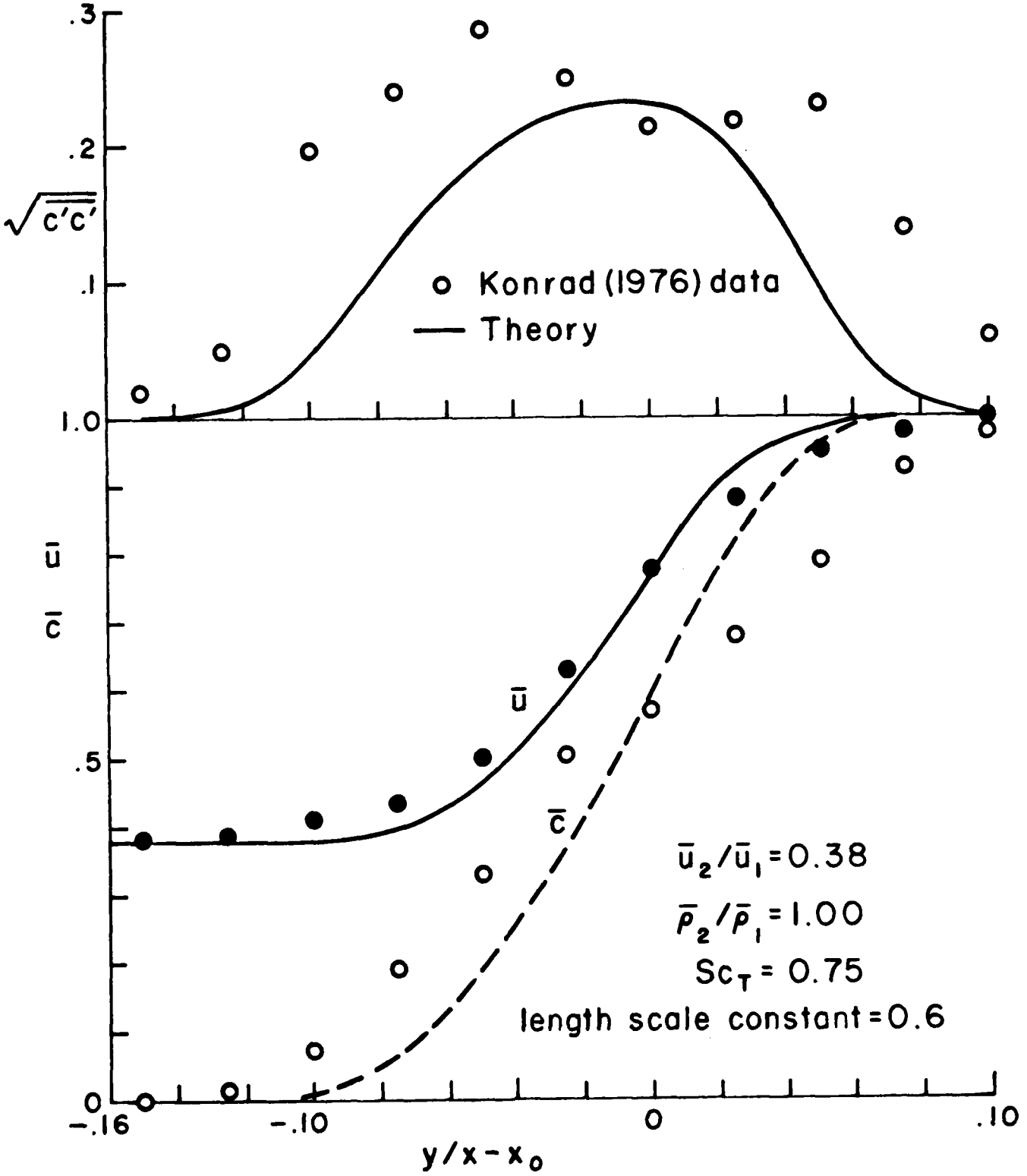

Figure 1. Mean velocity, mean species, and species correlation profiles in uniform density mixing layer.

This selection of the length scale leads to a prediction of $\sigma_0 = 9$. The calculated $\bar{u}$ profile is somewhat narrower than the experimental profile because of the low value of σ_0 reported by Konrad.

The differences in the mean velocity profile for this flow are slight. However, the differences in the mean species profiles are much larger. To match the experimental data of Konrad, it is necessary to increase the scale constant C to 0.7 and to reduce the turbulent Schmidt number Sc_T to 0.3 from its standard value of 0.75 (Lewellen, 1977). The effect of these changes on the calculations is shown in Figure 2.

The change required in the turbulent Schmidt number is quite large and is not supported by other comparisons with data for constant and nearly-constant density flows. Thus, Varma et al. (1977) have demonstrated good agreement with mean temperature axial decay rate data in a slightly heated planar jet using the A.R.A.P. models and $Sc_T = 0.75$. Lewellen (1976) has also shown good agreement with measurements in a heated two-dimensional wake using a scale equation formulation and $Sc_T = 0.75$. The required value of $Sc_T = 0.3$ seems extremely low and we feel additional data are required to justify model changes. There are data available on temperature profiles in a thermal mixing layer (Fiedler, 1974) that have recently come to our attention and this should provide additional information on the proper value of the scalar transport coefficients in a turbulent flow. The computed results for the species correlation $\overline{c'c'}$ in Figure 2 show that when good agreement with the mean quantities is secured, the fluctuation level is also in reasonable agreement with data.

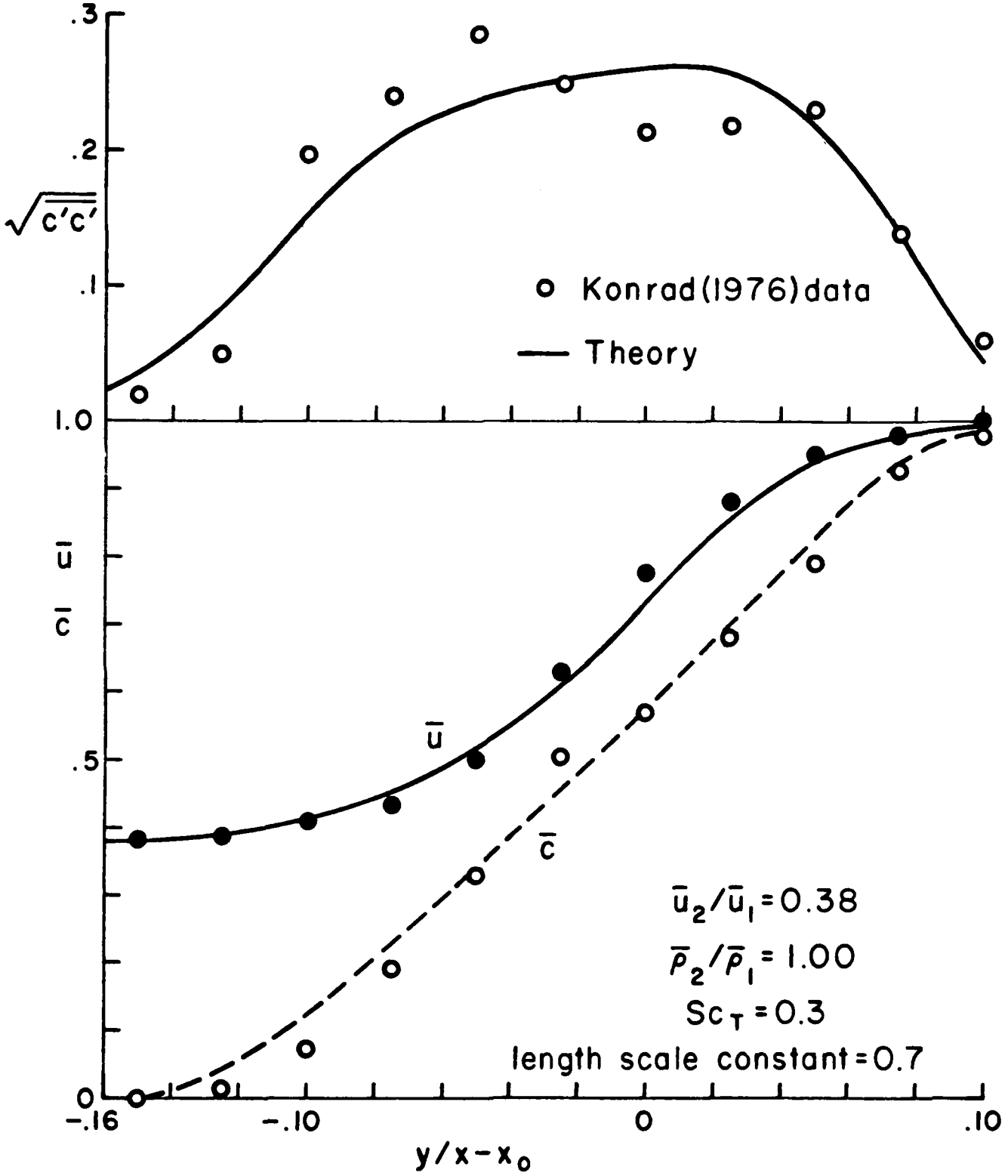

Figure 2. Mean velocity, mean species, and species correlation profiles in uniform density mixing layer with increased length scale constant and decreased turbulent Schmidt number.

This selection of the length scale leads to a prediction of $\sigma_o = 9$. The calculated $\bar{u}$ profile is somewhat narrower than the experimental profile because of the low value of σ_o reported by Konrad.

The differences in the mean velocity profile for this flow are slight. However, the differences in the mean species profiles are much larger. To match the experimental data of Konrad, it is necessary to increase the scale constant C to 0.7 and to reduce the turbulent Schmidt number Sc_T to 0.3 from its standard value of 0.75 (Lewellen, 1977). The effect of these changes on the calculations is shown in Figure 2.

The change required in the turbulent Schmidt number is quite large and is not supported by other comparisons with data for constant and nearly-constant density flows. Thus, Varma et al. (1977) have demonstrated good agreement with mean temperature axial decay rate data in a slightly heated planar jet using the A.R.A.P. models and $Sc_T = 0.75$. Lewellen (1976) has also shown good agreement with measurements in a heated two-dimensional wake using a scale equation formulation and $Sc_T = 0.75$. The required value of $Sc_T = 0.3$ seems extremely low and we feel additional data are required to justify model changes. There are data available on temperature profiles in a thermal mixing layer (Fiedler, 1974) that have recently come to our attention and this should provide additional information on the proper value of the scalar transport coefficients in a turbulent flow. The computed results for the species correlation $\overline{c'c'}$ in Figure 2 show that when good agreement with the mean quantities is secured, the fluctuation level is also in reasonable agreement with data.

Variable Density Shear Layer Studies

Analysis of Data. There is again a significant difference between the data of Brown and Roshko (1974) and Konrad (1976). The spread rate parameter σ_0 for the He - N_2 shear layer as calculated from Konrad data has a value of 7.4, that is, virtually the same σ_0 as for the uniform density shear layer. This does not support the conclusion of increased spreading rate for variable density flows with a high speed Helium stream configuration. The original Brown-Roshko data predicts $\sigma_0 \approx 8.8$, which indicates a 10 - 15% increase in the spreading rate compared to the uniform density data.

Second-Order Closure Calculations. The METREC program calculations have been carried out using the standard model constants with $Sc_T = 0.75$ and a length scale constant of 0.6. The predictions for both the mean velocity and mean species profiles are significantly narrower than the experimental data. The calculated spread rate $\sigma_0 \approx 13$. This requires modifications in our modeling of the dynamics of the turbulent flow and is under further study. The important variable is the turbulent macroscale. The development of a tensor length scale equation based on two-point correlation functions is underway at A.R.A.P. as part of other research efforts, and the same procedure should be useful in the calculation of the turbulent scales in variable-density flows.

We have also carried out calculations of the variable-density shear layer using two-equation turbulence models (kε2 model) and find similar

disagreement between the predicted and experimental mean profiles. Parker and Sirignano (1978) also report a factor of two error in the predicted shear layer width with a $k\varepsilon$ model compared to the Brown-Roshko data. The $k\varepsilon$ models and the A.R.A.P. second-order closure models have been used successfully for computations of other variable-density jet flows (see below) and the reasons for the disagreement with the shear layer data have to be understood. This, of course, must also include a reexamination of the available data and additional experimental measurements in variable-density flows.

The results for the species correlations, $\overline{c'c'}$, using the two pdf models are compared to the data in Figure 3. The error in the mean profiles has been taken into account by normalizing the results by the width of the mean species profile. The results for $\overline{c'c'}$ using the "typical eddy" pdf model are in better agreement with the data than the results obtained by using the "second-order approximation" procedure that neglects the higher-order scalar correlations. The results demonstrate the importance of modeling these correlations in the calculations.

Variable-Density Axisymmetric Jet Flow

The predictions of the METREC code for a hydrogen axisymmetric jet flow in a coflowing airstream are compared to the experimental measurements in Figure 4. The experimental data is by Chriss and Paulk (1972) and is Test Case 10 of the NASA Free Turbulent Shear Flows Conference data set. The hydrogen stream has a velocity of 1005 m/sec, and the velocity

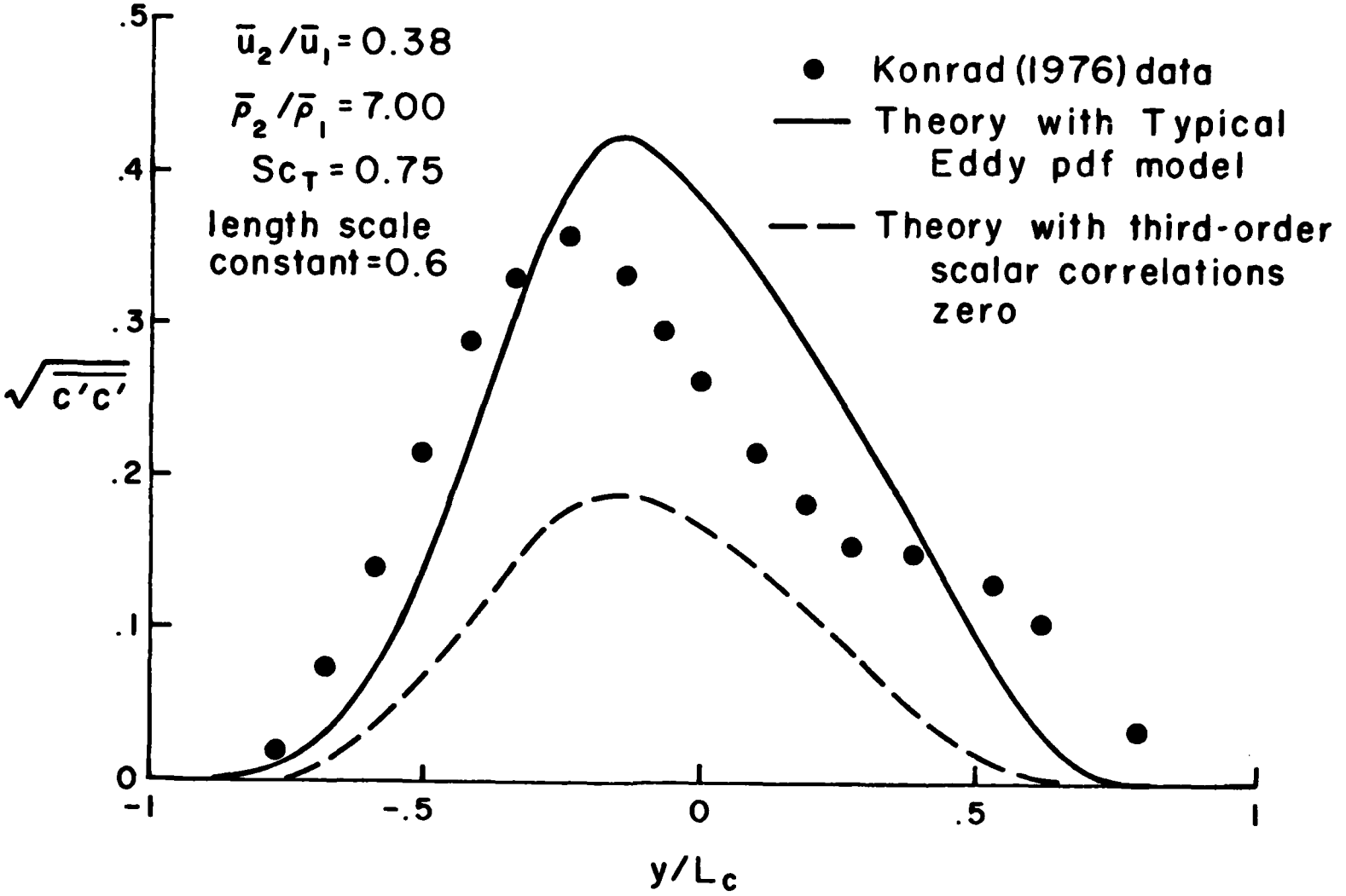

Figure 3. Species correlation profiles in variable density mixing layer.

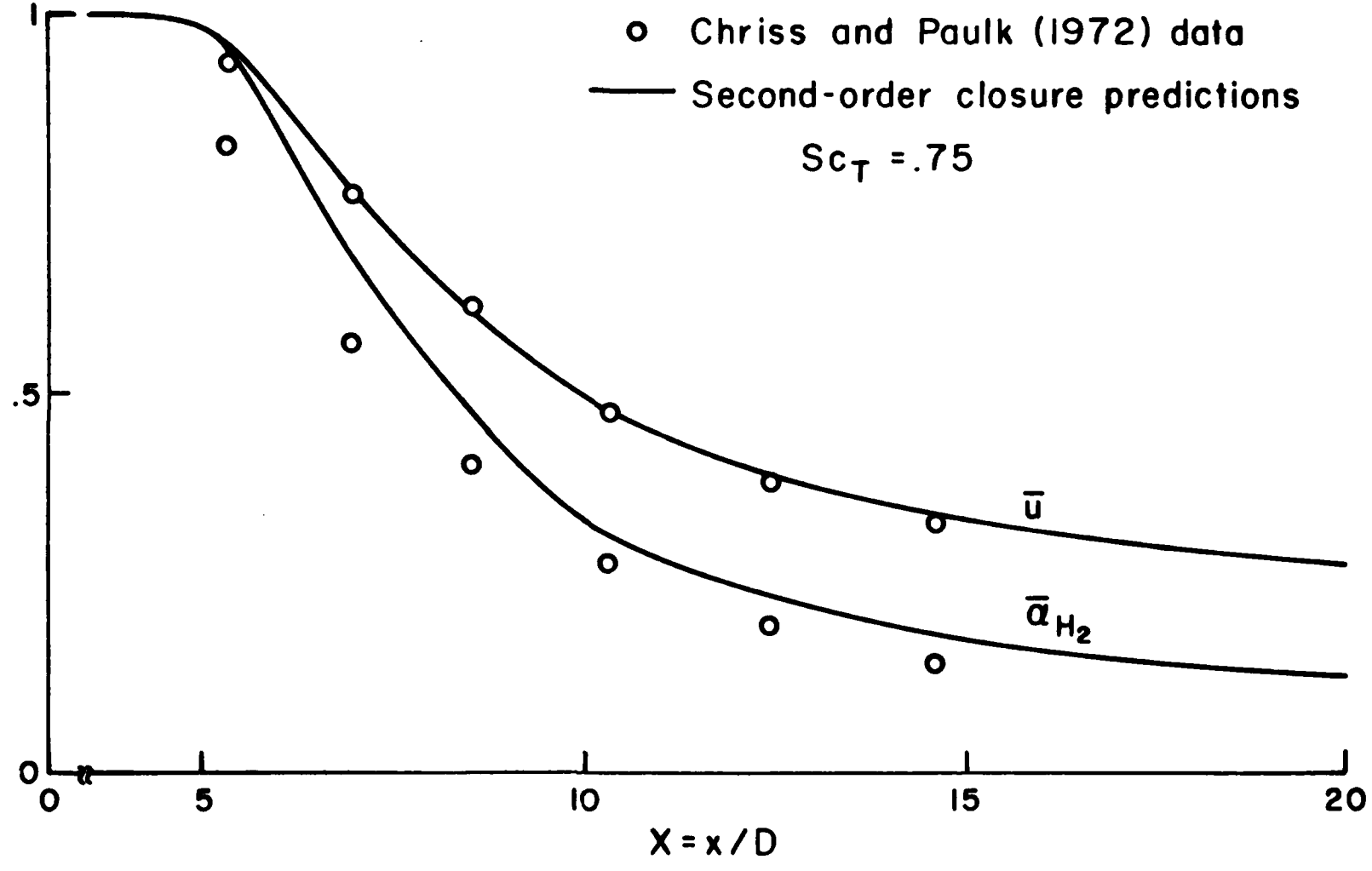

Figure 4. Axial decay of mean velocity and mean species mass fraction in a coflowing axisymmetric variable density jet flowfield.

ratio of hydrogen to air stream is 6.3. The density ratio at the nozzle exit is about 11. The calculations used a turbulent Schmidt number of 0.75. The calculations are started from given initial mean profiles at $x/D \approx 3$, The initial turbulence profiles are not provided. The calculations are started with a spot of turbulence at the initial station. The results in Figure 4 are obtained by using our standard procedure of selecting the turbulence level $\overline{u'u'} = .01\,\Delta\bar{u}^2$ at the initial station. In the near region of the flow, the results are somewhat sensitive to the initial turbulence level. Figure 4 compares the predicted centerline variation of the mean velocity and hydrogen mass fraction with the data. The agreement is quite satisfactory. For this flowfield the results obtained with the use of the "second-order approximation" are virtually the same as the results from the "typical eddy" model shown in Figure 4.

3. STATISTICAL CONSTRAINTS ON CORRELATIONS FOR THREE SPECIES FLOWFIELDS

Basic statistical principles are being used to obtain the rigorous bounds on correlations of various variables in a variable density three species flowfield. The procedures being used are similar to those developed during the derivation of constraints for a two species system (Varma et al., 1978). However, the three species system is far more complex and at present we have only succeeded in developing some of the bounds for the second-order correlations.

Consider a three species flow with constant pressure and temperature. Let α , β , and γ represent the mass fractions of the species. We are mainly interested in deriving the constraints on the following scalar moments: $\overline{\alpha}$, $\overline{\beta}$, $\overline{\alpha^2}$, $\overline{\beta^2}$, $\overline{\alpha\beta}$, $\overline{\alpha\rho}$, $\overline{\beta\rho}$, and $\overline{\rho^2}$. Additional constraints on various third-order moments will also be useful.

Given $\overline{\alpha}$ Only

We first assume that only $\overline{\alpha}$ is specified. Simple conservation relations lead to the following inequalities.

$$\boxed{0 \leq \overline{\alpha} \leq 1} \qquad (1)$$

$$\boxed{0 \leq \overline{\beta} \leq 1 - \overline{\alpha}} \qquad (2)$$

Use of the renormalization theorem and Cauchy-Schwarz inequality leads to

$$\boxed{\overline{\alpha}^2 \leq \overline{\alpha^2} \leq \overline{\alpha}} \tag{3}$$

$$0 \leq \overline{\alpha\beta} \leq \overline{\alpha} - \overline{\alpha^2} \tag{4}$$

$$0 \leq \overline{\beta^2} \leq \overline{\beta} - \overline{\alpha\beta} \tag{5}$$

Given just $\overline{\alpha}$, Eq. (3) represents the tightest bounds on $\overline{\alpha^2}$. Substituting the $\overline{\alpha^2}$ bounds in Eqs. (4) and (5) leads to

$$\boxed{0 \leq \overline{\alpha\beta} \leq \overline{\alpha}(1 - \overline{\alpha})} \tag{6}$$

$$\boxed{0 \leq \overline{\beta^2} \leq 1 - \overline{\alpha}} \tag{7}$$

These are the best bounds. The extremum values correspond to the *delta function* pdf's sketched below.

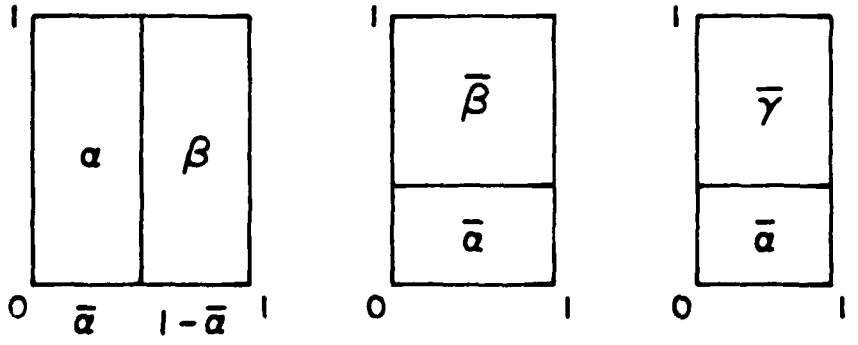

Given $\overline{\alpha}$ and $\overline{\beta}$

The conservation conditions lead to the following expressions.

$$0 \leq \overline{\alpha} \leq 1 - \overline{\beta} \tag{8}$$

$$0 \leq \overline{\beta} \leq 1 - \overline{\alpha} \tag{9}$$

We have previously derived the following bounds on $\overline{\alpha^2}$ and $\overline{\beta^2}$,

$$\boxed{\overline{\alpha}^2 \leq \overline{\alpha^2} \leq \overline{\alpha}} \tag{10}$$

$$\boxed{\overline{\beta}^2 \leq \overline{\beta^2} \leq \overline{\beta}} \tag{11}$$

It will now be shown that pdf's can be constructed that attain these extremum values. Therefore, the above represent the best bounds on the second-order moments.

For a three species system, the allowed phase space region for the pdf is represented by the triangle shown on the following page. The specification of $\overline{\alpha}$ and $\overline{\beta}$ corresponds to defining the location of the centroid. If the pdf corresponds to all the mass distribution concentrated at the centroid, the lower bounds on $\overline{\alpha^2}$ and $\overline{\beta^2}$ are attained.

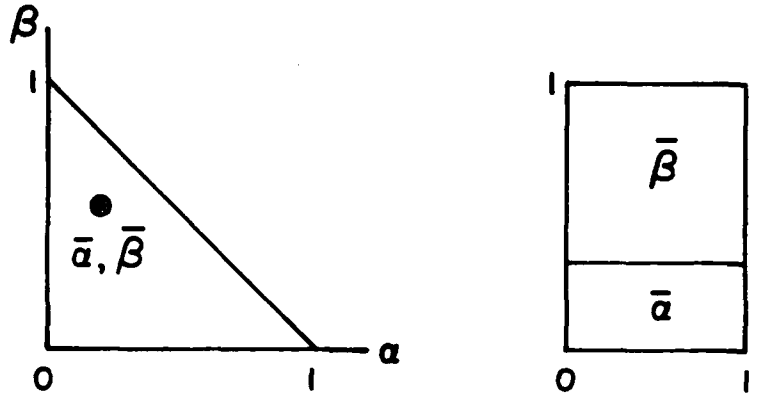

The upper bounds are attained by the following pdf's.

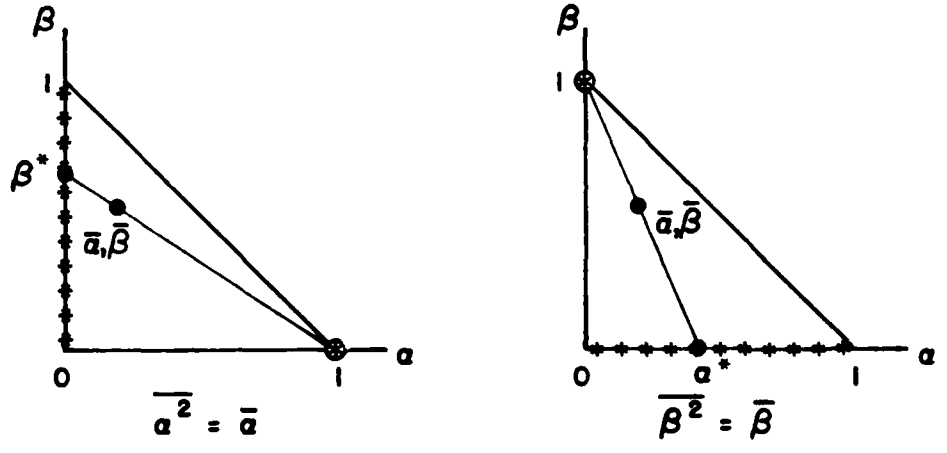

In the above diagrams, for generality we have considered a distribution of masses along the lines $\alpha = 0$ or $\beta = 0$, respectively. These mass distributions are such that for the figure on the left the centroid of the distribution along the line $\alpha = 0$ is located at β^*, the position corresponding to a straight line connecting $\alpha = 1$ and the given centroid. Similar considerations hold for the figure on the right.

The bounds on $\overline{\alpha\beta}$ are more interesting. Appendix A details the derivation of an upper bound on $\overline{\alpha\beta}$. Using this proof, we propose the following bounds on $\overline{\alpha\beta}$.

$$\boxed{0 \leq \overline{\alpha\beta} \leq \frac{\bar{\alpha} \cdot \bar{\beta}}{\bar{\alpha} + \bar{\beta}}} \tag{12}$$

If these values can be realized by physically realistic pdf's, then these are the tightest bounds on the correlation. The lower bound is attained by mass distributions that are restricted to the lines $\alpha = 0$ and $\beta = 0$.

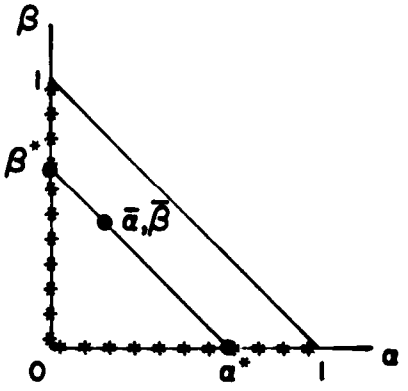

$$\overline{\alpha\,\beta} \equiv 0$$

The upper bound is realized by the following pdf.

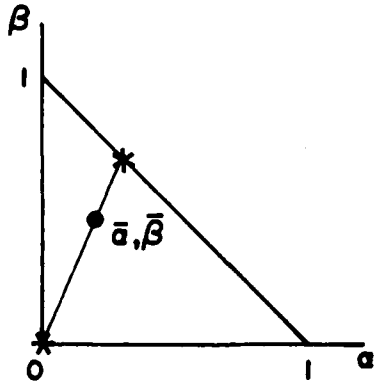

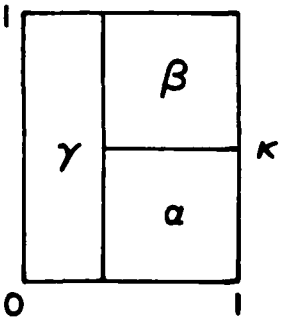

Therefore, the best bounds on $\overline{\alpha\beta}$ are as indicated in Eq. (12).

Given $\bar{\alpha}$, $\bar{\beta}$, and $\overline{\alpha^2}$ (or $\overline{\beta^2}$ or $\overline{\alpha\beta}$)

We now wish to determine the allowed regions for the ($\overline{\alpha^2}$, $\overline{\beta^2}$) space and for the ($\overline{\alpha^2}$, $\overline{\alpha\beta}$) space.

The independent bounds on $\overline{\alpha^2}$ and $\overline{\beta^2}$ define a rectangle in the ($\overline{\alpha^2}$, $\overline{\beta^2}$) domain. However, for certain specified values of the second-order moments, there are regions within the rectangle that must be excluded.

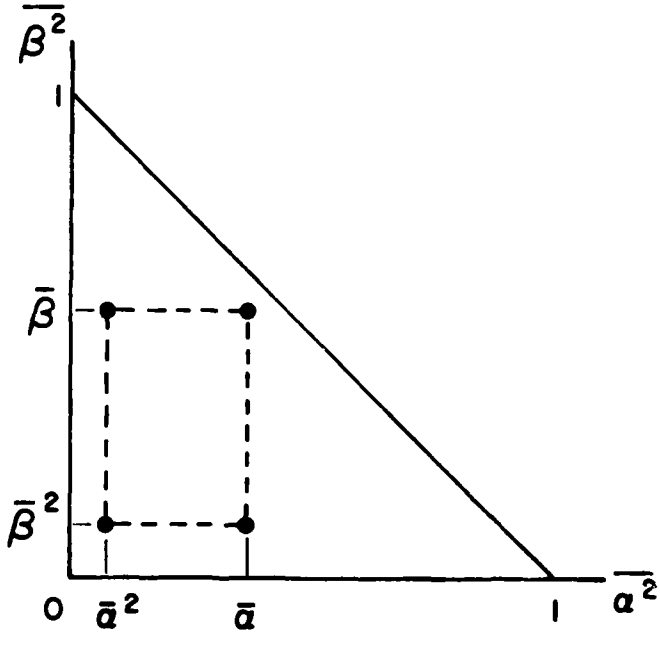

Consider $\overline{\alpha^2} = \bar{\alpha}$: To attain the upper bound on $\overline{\alpha^2}$, the distribution must have the form shown on the following page. We will calculate the smallest value of $\overline{\beta^2}$ that is allowed.

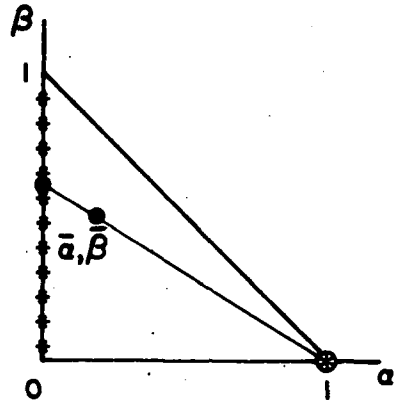

$$P(\alpha,\beta) = (1-\bar{\alpha})P_2(\beta)\delta(\alpha) + \bar{\alpha}\delta(\alpha-1)\delta(\beta)$$

$$\bar{\beta} = (1-\bar{\alpha})\int \beta P_2(\beta)d\beta$$

$$\overline{\beta^2} = (1-\bar{\alpha})\int \beta^2 P_2(\beta)d\beta$$

Cauchy-Schwarz inequality gives

$$\int \beta^2 P_2(\beta)d\beta \geq \left[\int \beta P_2(\beta)d\beta\right]^2$$

or

$$\frac{\overline{\beta^2}}{1-\bar{\alpha}} \geq \left(\frac{\bar{\beta}}{1-\bar{\alpha}}\right)^2$$

$$\overline{\beta^2} \geq \frac{\bar{\beta}^2}{1-\bar{\alpha}} \qquad (13)$$

Thus, $\overline{\beta^2} = \bar{\beta}^2$ cannot be reached for maximal $\overline{\alpha^2}$ and the lower right-hand corner of the rectangle is excluded.

Similarly, by reversing the roles of α and β, for $\overline{\beta^2} = \bar{\beta}$, the minimum $\overline{\alpha^2}$ allowed will be

$$\overline{\alpha^2} \geq \frac{\bar{\alpha}^2}{1 - \bar{\beta}} \tag{14}$$

The upper left-hand corner of the rectangle is not allowed.

Consider $\overline{\alpha^2} = \bar{\alpha}^2$: We wish to calculate how large $\overline{\beta^2}$ can be for the lower bound of $\overline{\alpha^2}$. The minimal value of $\overline{\alpha^2}$ is attained by the distribution sketched below on the left.

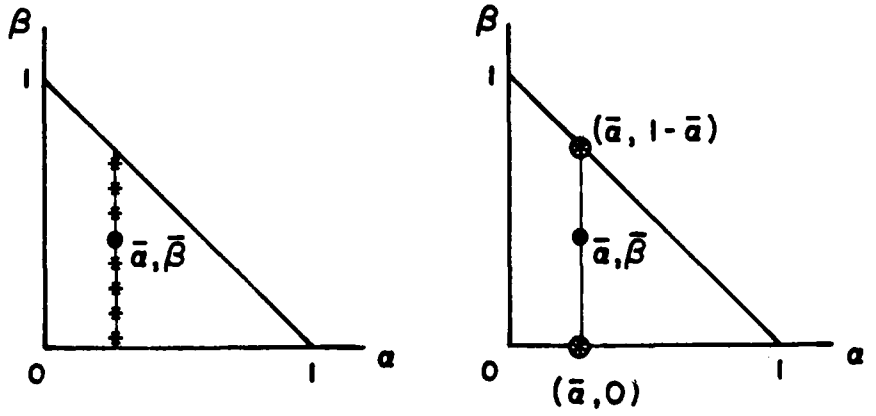

$$P(\alpha,\beta) = P_2(\beta)\delta(\alpha - \bar{\alpha})$$

$$\bar{\beta} = \int \beta P_2(\beta) d\beta$$

$$\overline{\beta^2} = \int \beta^2 P_2(\beta) d\beta$$

consider $P_2(\beta)$ to be a two delta function distribution with the delta functions located on the sides of the triangle (sketch on right).

$$P_2(\beta) = (1 - w)\delta(\beta) + w\delta[\beta - (1 - \bar{\alpha})]$$

$$\bar{\beta} = w(1 - \bar{\alpha}) \qquad w = \frac{\bar{\beta}}{1 - \bar{\alpha}}$$

$$\overline{\beta^2} = \frac{\bar{\beta}}{1 - \bar{\alpha}} (1 - \bar{\alpha})^2$$

$$\overline{\beta^2} = \bar{\beta}(1 - \bar{\alpha}) \tag{15}$$

It is postulated that $\overline{\beta^2}$ cannot be larger than this value for other mass distributions that are located in the interior region of the triangle. This has not yet been proven.

Similarly, for $\overline{\beta^2} = \overline{\beta}^2$, the largest allowed $\overline{\alpha^2}$ is

$$\overline{\alpha^2} = \overline{\alpha}(1 - \overline{\beta}) \tag{16}$$

With these derivations, the excluded sections of the rectangle are shown below. The other two corners of the rectangle are accessible by pdf's in which (i) a delta function is located at the centroid $(\overline{\alpha},\overline{\beta})$ and (ii) three delta functions are located at the three vertices of the triangle.

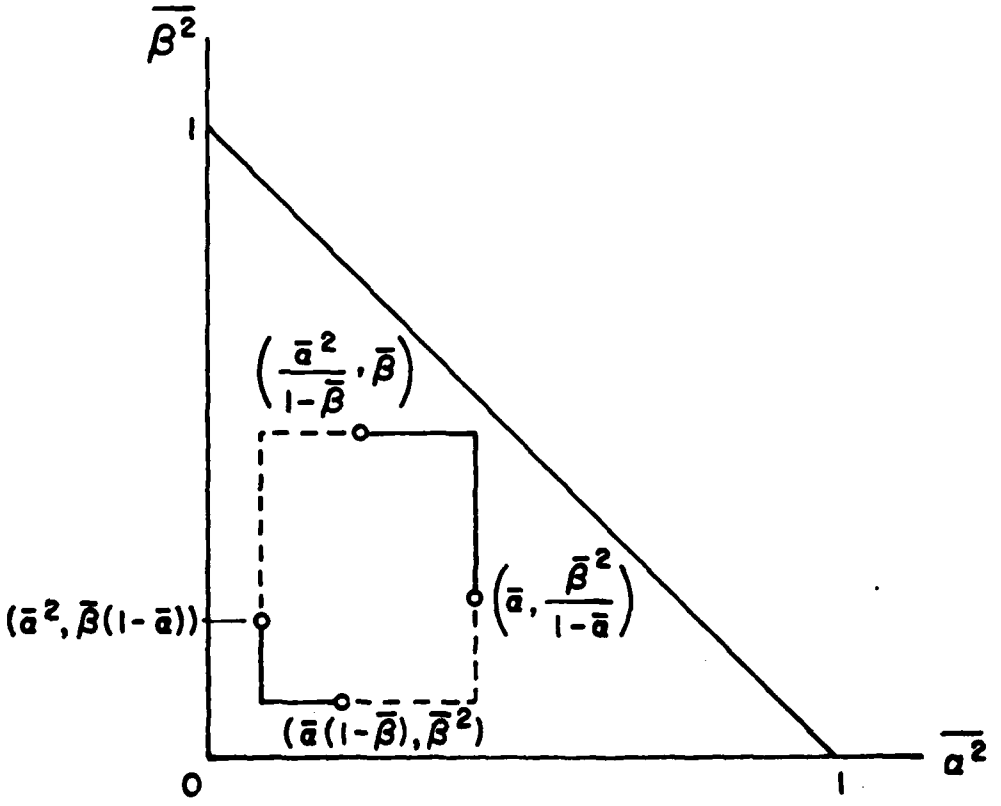

We have determined the shape of the connecting curves between the above points by considering a series of two delta function pdf's, with the delta functions located on the sides of the triangle. The line joining the delta function locations must pass through the specified centroid $(\bar{\alpha},\bar{\beta})$. The allowed region has been calculated for the special case $\bar{\alpha} = \bar{\beta} = 0.25$, and is shown in Figure 5. We have also sketched the expected shape of the allowed region for $\bar{\alpha} = 0.3$, $\bar{\beta} = 0.4$ on the same figure. There are some indications that these are the best bounds in $(\overline{\alpha^2},\overline{\beta^2})$ space, but we have not yet completed the proof for other more general mass distributions different from two delta functions located on the sides of the triangle.

Similar procedures have been used to determine the allowed region in $(\overline{\alpha^2},\overline{\alpha\beta})$ space. The independent bounds on $\overline{\alpha^2}$ and $\overline{\alpha\beta}$ define the following rectangle in the domain.

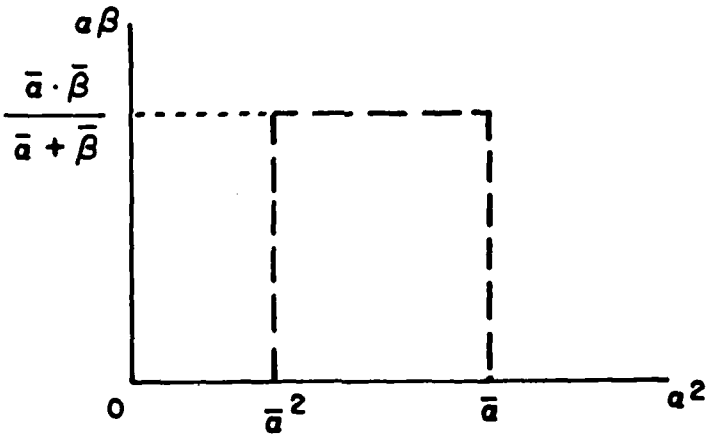

Consider $\overline{\alpha\beta} = 0$: We wish to obtain the bounds on $\overline{\alpha^2}$. For $\overline{\alpha\beta} = 0$, the pdf must be restricted to the $\alpha = 0$ and $\beta = 0$ sides of

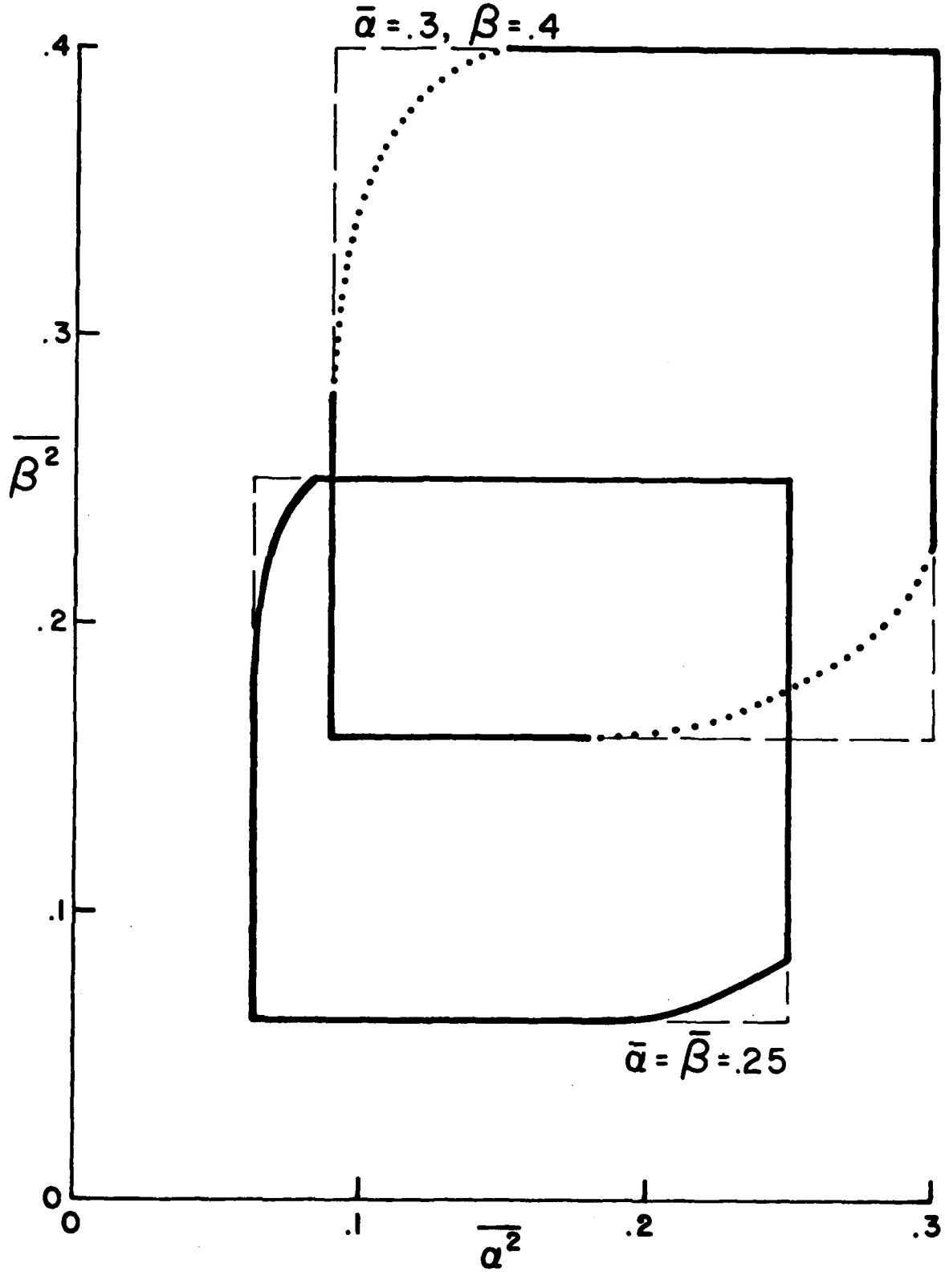

Figure 5. Statistical bounds on $\overline{\beta^2}$ and $\overline{\alpha^2}$ for specified $\bar{\alpha}$ and $\bar{\beta}$ in a three species system.

the triangle. We take a pdf composed of a delta function located at $(\alpha,0)$ and a general mass distribution on the line $\alpha = 0$.

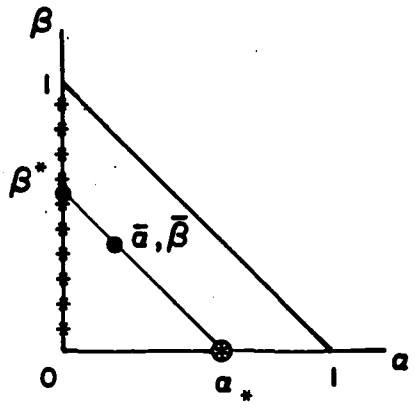

$$P(\alpha,\beta) = w\delta(\alpha)P_1(\beta) + (1-w)\delta(\beta)\delta(\alpha-\alpha_*)$$

$$\bar{\alpha} = (1-w)\alpha_*$$

$$\overline{\alpha^2} = (1-w)\alpha_*^2 = \bar{\alpha}\cdot\alpha_*$$

$$\alpha_* \geq \frac{\bar{\alpha}}{1-\bar{\beta}}$$

$$\overline{\alpha^2} \geq \frac{\bar{\alpha}^2}{1-\bar{\beta}} \qquad (17)$$

Consider $\overline{\alpha^2} = \bar{\alpha}$:

$$P(\alpha,\beta) = (1-\bar{\alpha})P_1(\beta)\delta(\alpha) + \bar{\alpha}\delta(\alpha-1)\delta(\beta)$$

$$\overline{\alpha\beta} = 0 \qquad (18)$$

The right-hand side of the rectangle is not allowed.

Consider $\overline{\alpha\beta} = \frac{\bar{\alpha}\cdot\bar{\beta}}{\bar{\alpha}+\bar{\beta}}$: For this limit the pdf must be

$$P(\alpha,\beta) = (1-\bar{\alpha}-\bar{\beta})\delta(\alpha)\delta(\beta) + (\bar{\alpha}+\bar{\beta})\delta\left(\alpha - \frac{\bar{\alpha}}{\bar{\alpha}+\bar{\beta}}\right)\delta\left(\beta - \frac{\bar{\beta}}{\bar{\alpha}+\bar{\beta}}\right)$$

Then,

$$\overline{\alpha^2} = (\bar{\alpha}+\bar{\beta})\left(\frac{\bar{\alpha}}{\bar{\alpha}+\bar{\beta}}\right)^2$$

or

$$\overline{\alpha^2} = \left(\frac{\bar{\alpha}^2}{\bar{\alpha}+\bar{\beta}}\right) \tag{19}$$

Consider $\overline{\alpha^2} = \bar{\alpha}^2$:

$$P(\alpha,\beta) = \delta(\alpha-\bar{\alpha})P_1(\beta)$$

$$\bar{\beta} = \int \beta P_1(\beta)d\beta$$

$$\overline{\alpha\beta} = \int \alpha\beta\delta(\alpha-\bar{\alpha})P_1(\beta)d\beta d\alpha$$

$$= \bar{\alpha}\int \beta P_1(\beta)d\beta$$

$$= \bar{\alpha}\cdot\bar{\beta} \tag{20}$$

Thus, the excluded regions of the rectangle in $(\overline{\alpha^2},\overline{\alpha\beta})$ space are shown below

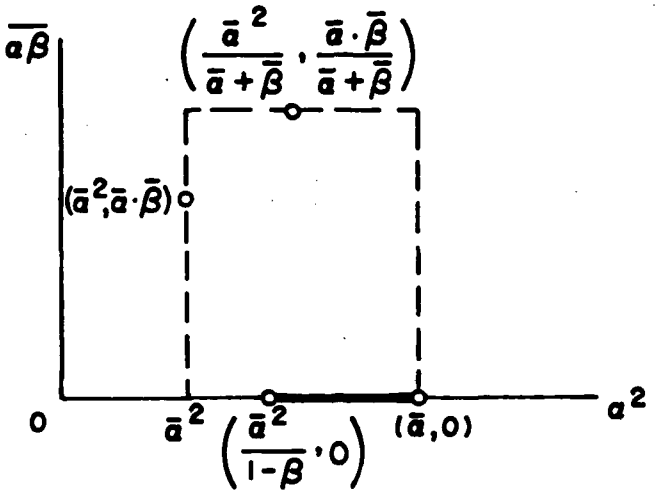

From Eq. (4), the general conservation bound on $\overline{\alpha\beta}$ is

$$0 \leq \overline{\alpha\beta} \leq \bar{\alpha} - \overline{\alpha^2}$$

For given $\bar{\alpha}$, the upper bound on $\overline{\alpha\beta}$ in $(\overline{\alpha^2},\overline{\alpha\beta})$ space is a straight line of slope -1. This represents a line joining the points $\left(\frac{\bar{\alpha}^2}{\bar{\alpha}+\bar{\beta}}, \frac{\bar{\alpha}\,\bar{\beta}}{\bar{\alpha}+\bar{\beta}}\right)$ and $(\bar{\alpha},0)$. The upper bound is attained by pdf distributions corresponding to two delta functions located on the sides $\alpha = 0$ and $\gamma = 0$.

The shapes of the connecting curve between the other allowed points can again be numerically calculated with the simplifying assumption of pdf's composed of two delta functions. The curve connecting the two top points has been calculated for $\bar{\alpha} = \bar{\beta} = 0.25$ and is plotted in Figure 6. The other curves still have to be calculated, but their expected behavior is shown in the figure.

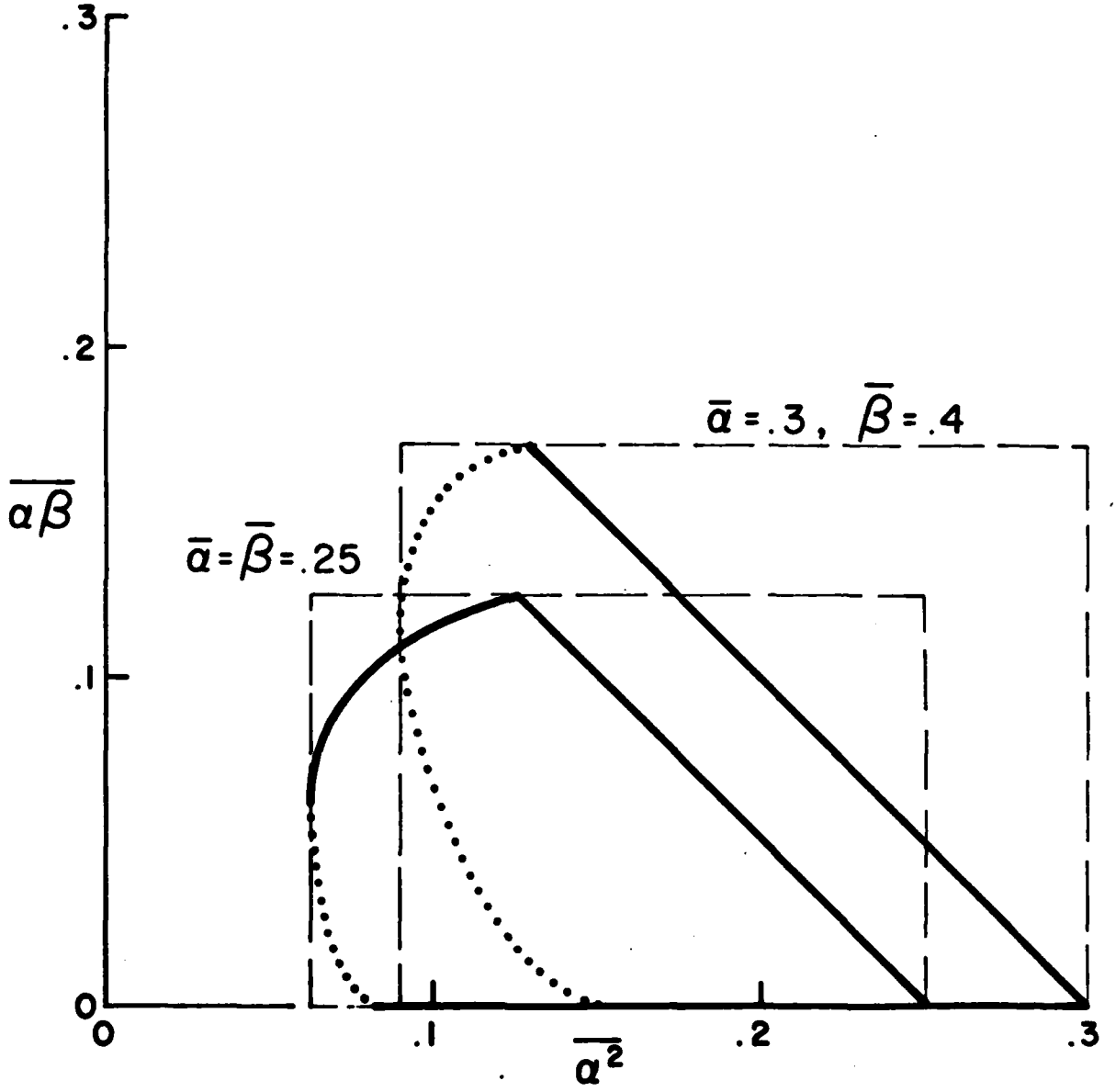

Figure 6. Statistical bounds on $\overline{\alpha\beta}$ and $\overline{\alpha^2}$ for specified $\bar{\alpha}$ and $\bar{\beta}$ in a three species system.

In summary, many of the important constraints on second-order correlations in a three species flow have been derived, and will prove useful in the testing of three species pdf models. Constraints on some correlations involving density fluctuations still remain to be developed along with the completion of some of the proofs discussed above.

4. CONCLUSIONS

Calculations have been made to compare the predictions of a second-order closure program with experimental measurements in uniform and variable density shear layers and jet flows. The studies for uniform density shear flows show good agreement for the mean velocity profiles and shear layer spread rate. The results for the mean species profiles are in good agreement with data when a turbulent Schmidt number of 0.3 is used. This is significantly lower than the value of 0.75 used in earlier studies, that are in good agreement with data for planar jets and wakes. Additional data on scalar profiles in shear layers will be useful to resolve this discrepancy. The results for variable density shear layer flows indicate the need for some improvement in the modeling of the dynamics of turbulence. The models appear to be satisfactory for variable density jet flows. The modeling of higher-order, scalar correlations using the "typical eddy" pdf model results in significant improvement in the prediction of second-order species correlations.

5. ACKNOWLEDGMENTS

The development of the statistical constraints on three species systems were mainly carried out by Drs. Mansfield and Sandri with support from the Air Force Office of Scientific Research under Contract Number F44620-76-C-0048.

6. REFERENCES

Birch, S.F. and Eggers, J.M. (1973): A Critical Review of the Experimental Data for Developed Free Turbulent Shear Layers. Free Turbulent Shear Flows, Volume I - Conference Proceedings, NASA SP-321, pp. 11-28.

Brown, G.L. and Roshko, A. (1974): On Density Effects and Large Structure in Turbulent Mixing Layers. J. Fluid Mech., Vol. 64, Part 4, pp. 775-816.

Chriss, D.E. and Paulk, R.A. (1972): An Experimentsl Investigation of Subsonic Coaxial Free Turbulent Mixing. AEDC-TR-71-236, AFOSR-TR-72-0237.

Fiedler, H.E. (1974): Transport of Heat Across a Plane Turbulent Mixing Layer. Advances in Geophysics, Vol. 18A, Academic Press, New York, N.Y., pp. 93-109.

Konrad, J.H. (1976): An Experimental Investigation of Mixing in Two-Dimensional Turbulent Shear Flows with Applications to Diffusion-Limited Chemical Reactions. Project SQUID Technical Report CIT-8-PU.

Lewellen, W.S., Teske, M.E., and Donaldson, C. duP. (1976): Variable Density Flows Computed by a Second-Order Closure Description of Turbulence. AIAA J., Vol. 14, No. 3, pp. 382-387.

Lewellen, W.S. (1977): Use of Invariant Modeling. Handbook of Turbulence, Vol. 1 (W. Frost and T.H. Moulden, eds.), Plenum Publishing Corp., pp. 237-280.

Parker, S.F. and Sirignano, W.A. (1978): A Numerical Study of Planar, Turbulent, Reacting Mixing Layers. Chemical and Physical Processes in Combustion, 1978 Fall Technical Meeting, The Combustion Institute, pp. 70-1 - 70-4.

Varma, A.K., Fishburne, E.S., and Beddini, R.A. (1977): Modeling of Turbulent Mixing and Reactions in Chemical Lasers. AFOSR-TR-77-0584.

Varma, A.K., Sandri, G., and Mansfield, P.J. (1978): Modeling of Scalar Probability Density Functions in Turbulent Flows. Project SQUID Technical Report ARAP-1-PU.

APPENDIX A

Consider a general pdf $P(\alpha,\beta)$ of the form

$$P(\alpha,\beta) = \sum_{i=1}^{n} w_i \delta(\alpha - \alpha_i)\delta(\beta - \beta_i)$$

with $0 \leq w_i \leq 1$, $0 \leq \alpha_i \leq 1$, $0 \leq \beta_i \leq 1$, $0 \leq \alpha_i + \beta_i \leq 1$, and $\sum w_i = 1$.

Then, to prove the inequality,

$$\overline{\alpha\beta} \leq \frac{\bar{\alpha}\,\bar{\beta}}{\bar{\alpha} + \bar{\beta}} \qquad (1)$$

The proof is by induction.

For $n = 1$:

$$P(\alpha,\beta) = w\delta(\alpha - \alpha_1)\delta(\beta - \beta_1)$$

$$\bar{\alpha} = w\alpha_1$$

$$\bar{\beta} = w\beta_1$$

$$\overline{\alpha\beta} = w\alpha_1\beta_1$$

Substituting in Eq. (1)

$$\alpha_1\beta_1 \leq \frac{\alpha_1\beta_1}{\alpha_1 + \beta_1}$$

or $\alpha_1 + \beta_1 \leq 1$, which is true!

We assume the result is true for $m = n - 1$.

$$M_{n-1} = \sum_{i=1}^{n-1} w_i$$

$$\frac{1}{M_{n-1}}\sum_{i=1}^{n-1}\alpha_i\beta_i w_i \leq \frac{\left(\frac{1}{M_{n-1}}\sum_{i-1}^{n-1}\alpha_i w_i\right)\left(\frac{1}{M_{n-1}}\sum_{j=1}^{n-1}\beta_j w_j\right)}{\frac{1}{M_{n-1}}\sum_{i=1}^{n-1}(\alpha_i + \beta_i)w_i}$$

or

$$\sum_{i=1}^{n-1}\alpha_i\beta_i w_i \leq \frac{\left(\sum_{i=1}^{n-1}\alpha_i w_i\right)\left(\sum_{j=1}^{n-1}\beta_j w_j\right)}{\sum_{i=1}^{n-1}(\alpha_i + \beta_i)w_i}$$

We then have,

$$\overline{\alpha\beta} = \sum_{i=1}^{n-1} \alpha_i \beta_i w_i + \alpha_n \beta_n w_n$$

$$\leq \frac{\left(\sum_{i=1}^{n-1} \alpha_i w_i\right)\left(\sum_{j=1}^{n-1} \beta_j w_j\right)}{\sum_{i-1}^{n-1} (\alpha_i + \beta_i) w_i} + \alpha_n \beta_n w_n$$

Then we wish to prove:

$$\frac{\left(\sum_{i=1}^{n-1} \alpha_i w_i\right)\left(\sum_{j=1}^{n-1} \beta_j w_j\right)}{\sum_{i=1}^{n-1} (\alpha_i + \beta_i) w_i} + \alpha_n \beta_n w_n \leq \frac{\left(\sum_{i=1}^{n} \alpha_i w_i\right)\left(\sum_{j=1}^{n} \beta_j w_j\right)}{\sum_{i=1}^{n} (\alpha_i + \beta_i) w_i} \qquad (2)$$

Define

$$A \equiv \sum_{i=1}^{n-1} \alpha_i w_i \qquad B = \sum_{j=1}^{n-1} \beta_j w_j$$

$$a = \alpha_n \qquad b = \beta_n \qquad c = w_n$$

Eq. (2) is equivalent to showing

$$\frac{AB}{A + B} + abc \leq \frac{(A + ac)(B + bc)}{A + ac + B + bc} \tag{3}$$

This can be simplified to

$$(A + B)ab(A + B + ac + bc) \leq A(Ab + abc) + B(Ba + abc) \tag{4}$$

Define

$$f(c) = (A + B)ab(A + B + ac + bc) - A(Ab + abc) - B(Ba + abc)$$

A , B , a , and b are independent of c and hence f is linear in c .

To prove inequality (4) is equivalent to showing that $f(0) \leq 0$ and $f'(0) \leq 0$.

$$f(0) = (A + B)^2ab - A^2b - B^2a$$

Lemma 1

$$f(0) \leq 0$$

$$(A + B)^2ab \leq A^2b + B^2a \tag{5}$$

Proof of Lemma

If a or b is zero, the conclusion is trivial.

Assume $a \neq 0$, $b \neq 0 \rightarrow a < 1$, $b < 1$

$$(A + B)^2 \leq A^2 \frac{1}{a} + B^2 \frac{1}{b}$$

Let $x = \frac{1}{a}$, $y = \frac{1}{b}$

$$a < 1 \rightarrow x = 1 + \varepsilon_1 \quad \text{for some} \quad \varepsilon_1 > 0$$

$$b < 1 \rightarrow y = 1 + \varepsilon_2 \quad \text{for some} \quad \varepsilon_2 > 0$$

$$a + b \leq 1 \rightarrow \frac{1}{x} + \frac{1}{y} \leq 1$$

or

$$\frac{1}{1 + \varepsilon_1} + \frac{1}{1 + \varepsilon_2} \leq 1$$

or

$$1 \leq \varepsilon_1 \cdot \varepsilon_2$$

Now to prove,

$$(A + B)^2 \leq A^2(1 + \varepsilon_1) + B^2(1 + \varepsilon_2)$$

or

$$2AB \leq A^2\varepsilon_1 + B^2\varepsilon_2$$

consider,

$$(A\sqrt{\varepsilon_1} - B\sqrt{\varepsilon_2})^2 \geq 0$$

$$A^2\varepsilon_1 + B^2\varepsilon_2 \geq 2AB\sqrt{\varepsilon_1\varepsilon_2}$$

$$\geq 2AB \text{ as } \sqrt{\varepsilon_1\varepsilon_2} \geq 1$$

This proves the lemma.

Lemma 2

$$f'(0) \leq 0$$

$$f'(0) = (A + B)ab(a + b) - Aab - Bab$$

$$f'(0) = ab(A + B)(a + b - 1)$$

$$a + b - 1 \leq 0$$

$$\therefore \qquad f'(0) \leq 0$$

The proof is complete.

$$\overline{\alpha\beta} \leq \frac{\overline{\alpha}\,\overline{\beta}}{\overline{\alpha} + \overline{\beta}} \quad .$$

Unclassified

SECURITY CLASSIFICATION OF THIS PAGE (When Data Entered)

REPORT DOCUMENTATION PAGE

READ INSTRUCTIONS BEFORE COMPLETING FORM

(14) SQUID-ARAP-2-PU

2. GOVT ACCESSION NO. AD-A083 723

3. RECIPIENT'S CATALOG NUMBER

(6) 4. TITLE (and Subtitle)

Second-Order Closure Modeling of Variable Density Turbulent Flows

5. TYPE OF REPORT & PERIOD COVERED

6. PERFORMING ORG. REPORT NUMBER

(10) 7. AUTHOR(s)

Ashok K. Varma Peter J. Mansfield Guido Sandri

(15) 8. CONTRACT OR GRANT NUMBER(s)

N00014-75-C-1143

9. PERFORMING ORGANIZATION NAME AND ADDRESS

Aeronautical Research Associates of Princeton, Inc.
50 Washington Road, P.O. Box 2229
Princeton, NJ 08540

10. PROGRAM ELEMENT, PROJECT, TASK AREA & WORK UNIT NUMBERS

NR-098-038

11. CONTROLLING OFFICE NAME AND ADDRESS

ONR-Power Program through Purdue University,
West Lafayette, Indiana 47907

(11) 12. REPORT DATE

Mar[illegible]79

(12) 44

13. NUMBER OF PAGES

49

14. MONITORING AGENCY NAME & ADDRESS(if different from Controlling Office)

Office of Naval Research, Power Program, Code 473
Department of the Navy
800 No. Quincy Street
Arlington, VA 22217

15. SECURITY CLASS. (of this report)

Unclassified

15a. DECLASSIFICATION/DOWNGRADING SCHEDULE

16. DISTRIBUTION STATEMENT (of this Report)

This document has been approved for public research and sale; its distribution is unlimited.

17. DISTRIBUTION STATEMENT (of the abstract entered in Block 20, if different from Report)

Same (9) Technical rpt.

18. SUPPLEMENTARY NOTES

19. KEY WORDS (Continue on reverse side if necessary and identify by block number)

Turbulence modeling
Variable density flows
Second-order closure
Reactive flows
Combustors

20. ABSTRACT (Continue on reverse side if necessary and identify by block number)

Mixing and Chemical reactions under turbulent flow conditions are a basic feature of the energy release processes in many combustion and propulsion systems. The development of predictive calculation procedures for these systems requires the understanding and modeling of coupling between turbulence and various physical and chemical processes. Second-order closure modeling of turbulent flows provides a rational framework for studying these interactions.

Models for the scalar probability density function (pdf) have to be (over)

DD FORM 1 JAN 73 1473 EDITION OF 1 NOV 65 IS OBSOLETE
S/N 0102-LF-014-6601

Unclassified 403 617 next page

SECURITY CLASSIFICATION OF THIS PAGE (When Data Entered)

cont.

developed to achieve closure of turbulent transport equations for mixing and reacting flows. A delta function "typical eddy" pdf model for two species flows has been developed and incorporated into a complete second-order closure computer program. The program has been used to study uniform and variable density flowfields and the model predictions have been compared to experimental measurements. The modeling of turbulence dynamics for variable density flows requires further improvement. However, the importance of modeling the higher-order scalar correlations has been demonstrated.

A number of statistical constraints on three species flowfields have also been derived. These will be useful in the development of the "typical eddy" pdf model for reacting flows.